Mutual activation of the epithelial-to-mesenchymal transition and metabolic reprogramming stabilizes hybrid phenotypes with high metastatic potential

Madeline Galbraith[1], Dongya Jia[2], Herbert Levine[3], and José Onuchic[1]

[1]Center for Theoretical Biological Physics, Rice University, Houston, TX, USA

[3]Center for Theoretical Biological Physics, Department of Physics, and Department of Bioengineering, Northeastern University, Boston, MA, USA

Abstract

Abnormal metabolism and attaining motility are two hallmarks of cancer. During metastasis, a developmental program, epithelial-to-mesenchymal transition (EMT) is often used by cancer cells to become motile. Aside from complete EMT, cancer cells can alternatively acquire a hybrid Epithelial/Mesenchymal (E/M) phenotype, which in many cases may be the primary instigator of metastasis. In addition, when leaving the primary tumor and entering blood circulation, cancer cells can increase their mitochondrial respiration without compromising their glycolytic activity, thus entering a hybrid metabolic mode using both oxidative phosphorylation (OXPHOS) and glycolysis. Understanding the relationship between cancer metabolism and EMT can therefore offer novel anti-metastasis strategies. Here, we analyze the relationship between metabolism and EMT by coupling their corresponding core decision-making molecular networks – AMPK/HIF-1/ROS and miR-34/SNAIL/miR-200/ZEB, respectively. We systematically elucidate how different phenotypes during EMT (E, M and hybrid E/M) are associated with different metabolic phenotypes (OXPHOS, glycolysis and hybrid (W/O) glycolysis/OXPHOS). Specifically, we identified the feedback loops that lead to the coupling of the hybrid E/M state with the mixed metabolic state – a potentially highly aggressive phenotype (E/M-W/O).

Strikingly, we found that even if the individual molecular network of EMT or metabolism does not support a hybrid phenotype, crosstalk can promote the existence of such a double hybrid phenotype. In this case, the state is created sequentially by first stabilizing the hybrid metabolic phenotype and then the hybrid E/M state, suggesting that metabolic reprogramming may be the primary driver behind the acquisition of highly aggressive cells.

Introduction

Metastasis remains the leading cause of cancer-related deaths[1] and thus it is critical to understand the physiological properties of cells that migrate from the primary tumor and initiate metastatic lesions. Typically, these properties have been studied one at a time. For example, cell motility is assumed to be related to the epithelial-to-mesenchymal transition (EMT). During EMT, the cells progressively lose cell-cell adhesion and apical-basal polarity, and increase their capacity for migration, invasion, and resistance to immune response [2,3]. The EMT has consistently been implicated in cells acquiring metastatic potential [4,5], and also plays a role in therapeutic resistance [6]. Recently, the bimodal picture of EMT has been superseded by a more complex scenario involving the hybrid epithelial/mesenchymal (E/M) phenotype which exhibits combined traits of epithelial (cell-cell adhesion) and mesenchymal (invasion) at the single-cell level. The hybrid E/M cells migrate collectively as a cluster and may account for the majority of metastases [7–10]. The existence of a hybrid E/M state has since been experimentally verified both in vitro (in many cancer cell lines) and in vivo (e.g. using a genetic mouse model of squamous cell carcinoma) and has been shown to be associated with therapy resistance alongside with poor survival rates [11–14]. Most importantly, these states appear to the most capable of initiating metastatic growth[15,16]. Fully understanding the behavior of the hybrid E/M phenotype is still an active area of research.

Metabolic reprogramming, another hallmark of cancer, enables cancer cells to adjust their metabolic activity for biomass and energy supply to survive in hostile environments [1,17]. Cells typically utilize oxidative phosphorylation (OXPHOS) under normoxic conditions and glycolysis when there is a lack of oxygen. However, cancer cells often prefer glycolysis even when oxygen is available, referred to as the Warburg effect or aerobic glycolysis [18,19]. During metastasis, cancer cells must be able to survive in different environments, resulting in these cells switching between different types of metabolism [20–23]. Metabolic reprogramming, specifically in the context of switching between the OXPHOS and Warburg metabolic phenotypes, can lead to mixed metabolic states [24–26] including a metabolic inactive low-low phenotype associated with therapy resistance in melanoma [27] and a hybrid glycolysis/OXPHOS phenotype associated with high metastatic potentials[24,28]. The hybrid glycolysis/OXPHOS phenotype has been observed in circulating tumor cells (CTCs) originating from breast tumors formed by 4T-1 cells [29]. The high metastatic potential of cancer cells with a hybrid metabolic phenotype has been confirmed in a number of additional experimental studies [28,30].

As already mentioned, systems biology approaches have typically focused separately on EMT and on metabolic plasticity. However, it has become increasingly clear that there exists extensive crosstalk between EMT and metabolism[30]. This crosstalk between EMT and metabolic reprogramming is important to metastasis and tumor proliferation [30–33]. Recent studies show that metabolic reprogramming can increase metastatic potential and drive EMT, or conversely that induction of EMT can drive metabolic reprogramming [34–37]. The underlying mechanisms of interaction between EMT and metabolic reprogramming remain poorly understood, with several competing hypotheses as discussed below. Kang et al have suggested cancer cells typically first undergo metabolic reprogramming then trigger EMT [38,39]; this

coupling, presumably, is a consequence of changes in the tumor microenvironment fostering metabolic reprogramming which drives EMT[40–42]. Another hypothesis is that there is mutual activation of EMT and metabolic reprogramming such that the most flexible phenotypes (hybrid E/M and hybrid glycolysis/OXPHOS (W/O)) become coupled, leading to a greatly increased metastatic potential[30]. This connection between EMT and metabolic reprogramming has recently been noticed in CTCs, which were shown to have high levels of both OXPHOS and glycolysis[29] and have also been shown to mainly consist of hybrid E/M cells, especially at high levels of NRF2, an antioxidation regulator[43]. Consistent coupling of EMT states and metabolic states has been seen in breast cancer stem cells (BCSCs). Specifically, the hybrid E/M-like BCSCs (E/M-BCSCs) have higher levels of OXPHOS and glycolysis as compared to the mesenchymal-like breast cancer stem cells (M-BCSCs) [44,45]. Thus, while there have been preliminary indications of the coupling of EMT states and metabolic states there is still much to be explored.

To decode the coupled decision-making of EMT and metabolism, we created a computational model which connects the core gene regulatory circuit underlying EMT – miR-34/SNAIL/miR-200/ZEB [7] and a recently proposed core circuit involved in metabolic reprogramming – AMPK/HIF-1/ROS [25]. We found that ROS is a key promoter of a possible "double-hybrid" state, namely a hybrid E/M state coupled with a mixed metabolic phenotype (hybrid E/M-W/O state). Additionally, HIF-1 may play a more central role in metabolic reprogramming driving EMT than AMPK. Also, when crosstalks between the circuits are active in both directions (EMT regulating metabolism, and vice versa), there are parameter space regions for which the hybrid E/M-W/O state is the only accessible state. Interestingly, if the parameters of the system were modified to exclude the hybrid states when the crosstalks are

inactive (i.e., neither the E/M or W/O states are initially accessible), once active, the crosstalks are able to modulate the phase space to generate the hybrid states. In fact, a single crosstalk is sufficient for the metabolic or EMT circuits to gain tristability. We also confirmed the roles of phenotypic stability factors (PSFs) of the hybrid E/M state - GRHL2 and OVOL2 [14,46], which further stabilized the hybrid E/M-W/O state for all sets of active crosstalks. Our results therefore suggest that a highly aggressive plastic phenotype along both the EMT and metabolic axes is a likely choice for a subset of cancer cells and, speculatively, may be critical for the metastatic process.

Model: Coupling the core EMT and metabolic networks

While the mechanisms of EMT and cancer metabolism have been investigated individually, the crosstalk between the two circuits and how the phenotypes are correlated is still largely unknown. Here we couple our previously studied regulatory networks of EMT [7] and metabolism [25]; see Figure 1A for the coupled network. Generally speaking, our combined model considers feedback loops that couple the two individual regulatory networks. The crosstalk between the EMT circuit and the metabolism circuit is either direct or indirect, the latter arising because our formulation focuses only on a few core components and effective interactions between them that can occur via intermediate reactants. We initially focus on the core networks and investigate the role of crosstalk. One question of interest is whether these crosstalks are sufficient to generate hybrid states. Lastly, we evaluate the role of PSFs OVOL and GRHL2 to investigate their effect on the stability of the E/M-W/O state.

The core EMT network is comprised of the transcription factors (TFs), ZEB and SNAIL, and the microRNA families, μ_{200} and μ_{34}. It is modeled as a translation-transcription chimeric circuit[7]. For a two-component chimeric circuit, the binding/unbinding dynamics are given by

$$\frac{d\mu}{dt} = g_\mu \mu - mY_\mu(\mu) - k_\mu \mu \quad (1)$$

$$\frac{dm}{dt} = g_m - mY_m(\mu) - k_m m \quad (2)$$

$$\frac{dB}{dt} = g_B mL(\mu) - k_B B \quad (3)$$

where the three functions Y_μ, Y_m, and L which represent respectively the active miRNA degradation rate, active mRNA degradation rate, and translation rate (details in SI section 1.1, Fig. S1-S3). The activation and inhibition of SNAIL and ZEB are mathematically represented as a shifted Hill function[47],

$$H(X, X_0, n_X, \lambda) = \lambda + \frac{1-\lambda}{1+(X/X_0)^{n_X}} \quad (4)$$

Once the threshold of the regulator (X_0) is achieved, the fold change (λ) represents the magnitude of the activation (λ >1) or inhibition (λ <1), and the sensitivity to the changes in X is represented by the Hill coefficient n (Fig. S3). Previous investigation of the core EMT network by Lu and collaborators examined sub-modules of the network and various parameter ranges. They determined the miR-200/ZEB module was responsible for the tristability of the system whereas the miR-34/SNAIL module acted as a noise buffer[7]. Additionally, the phenotypes of the tristable EMT network were correlated with the expression of miR-200 and ZEB mRNA; epithelial (E) with high miR-200/low ZEB, mesenchymal (M) with low miR-200/high ZEB, and E/M with intermediate miR-200/ZEB (see Fig. 1B, and section S2.1 for nullcline analysis).

In a separate line of investigation, a proposed core metabolism network - AMPK/HIF-1/ROS, gave insight into mixed metabolic modes of glucose metabolism. In this circuit, the regulation of the production and degradation terms are mathematically represented as shifted Hill functions. Within the metabolic regulatory network, there is also competitive regulation of ROS by HIF-1 and AMPK, which is modeled by a competition function similar to the shifted Hill function (details and functional form in SI section 1.2). Through this reduced circuit, Yu and collaborators were able to recover typical metabolic behavior of cancers and also identify a mixed metabolic (W/O) phenotype[25]. The tristable metabolic network has the metabolic phenotypes; OXPHOS (O) high AMPK/low HIF-1, aerobic glycolysis (W) low AMPK/high HIF-1, and mixed metabolism (W/O) intermediate AMPK/HIF-1 (see Fig. 1C).

To couple the core EMT and metabolic networks we identified crosstalks between our core components (see Fig. 1A). Starting with miRNA-based crosstalk links, the ability of a cell to eliminate ROS is reduced by μ_{34} via targeting and downregulating the NRF2-dependent antioxidant capability, [48–50]. ROS production may also be upregulated through μ_{34} downregulating SOD2 [51] or via the p53 pathway [52,53]. This increase in ROS levels is potentially more pronounced for mitochondrial ROS (mtROS) versus NADPH oxidase mediated ROS (noxROS) [48] and has recently been indicated as a factor in cancer drug resistance [54]. Next, crosstalk between HIF-1 and μ_{200} family members can either upregulate or downregulate Hif1 expression [55]. While miR-429 upregulates HIF-1, both miR-200b [56] and miR-200c [57] downregulate HIF-1 expression. Furthermore, there is a negative regulatory feedback loop between miR-200b and HIF-1[56]. The inhibition of miR-200b by HIF-1 is indirect, acting through upregulation of the downstream target ASCL2 [56]. Our coupled model includes a mutual inhibitory feedback between μ_{200} and HIF-1. Additionally, HIF-1 can upregulate SNAIL

[58]. The production of SNAIL is also a downstream target of AMPK. Once FOXO3 is activated by AMPK, it represses the production of SNAIL[59]. Similarly, ZEB is a downstream target of AMPK, and ZEB production is inhibited by FOXO [60,61]. Additionally, CREB, after being activated by AMPK via phosphorylation, can transcribe μ_{200} resulting in the upregulation of μ_{200}[62–66]. Please refer to supplementary Table S5 for a detailed description of all crosstalks that have been included in our modeling framework.

The new model we propose here is built by including these crosstalk links so as to couple the two core circuits of EMT and metabolic control respectively. We modify the metabolic circuit such that the mathematical model includes the miRNA regulation of HIF-1 by μ_{200} and confirm that the nullclines and expression of AMPK/HIF-1/ROS for the modified metabolic network model is consistent with results from the model detailed in Ref. [25] (Fig. S4). The full equations for the dynamics of all components of the circuit are given in SI Section 1.3 and the parameters along with a brief explanation are given in SI Section 1.4.

Assume that we have chosen parameters such that both the EMT and metabolic networks are tristable. This means that when the crosstalk links are inactive, there are nine possible combinations of the EMT and metabolic phenotypes: E-W, E-O, E-W/O, M-W, M-O, M-W/O, E/M-W, E/M-O, and E/M-W/O (Fig. 1D, details of numerical integration using the Euler method are given in section S2.2). By including active crosstalks, we can identify how the components of the networks interact and which EMT states and metabolic states become coupled.

While the Warburg state is characterized as high HIF-1/low AMPK and the epithelial state is characterized as high μ_{200}/low ZEB mRNA expression, adding the new links will quantitatively alter the expression profiles for the various steady states. This means that the use

of fixed thresholds to determine the state of the cell is no longer appropriate. Therefore, we use a distance metric normalized by the expression of the decoupled network to classify the generated expression profiles as indicative of one of the nine coupled states (see Section S2.3 for details). With our baseline decoupled network parameters, we show that 1000 initial conditions are large enough to generate consistent percentages of different states (Fig. S5-S7) - with the hybrid state being most populous (W/O and E/M) followed by the W and M phenotypes, followed by the O and E states. This result is just for one set of parameters and others will lead to a different fraction of initial conditions leading to these disparate states.

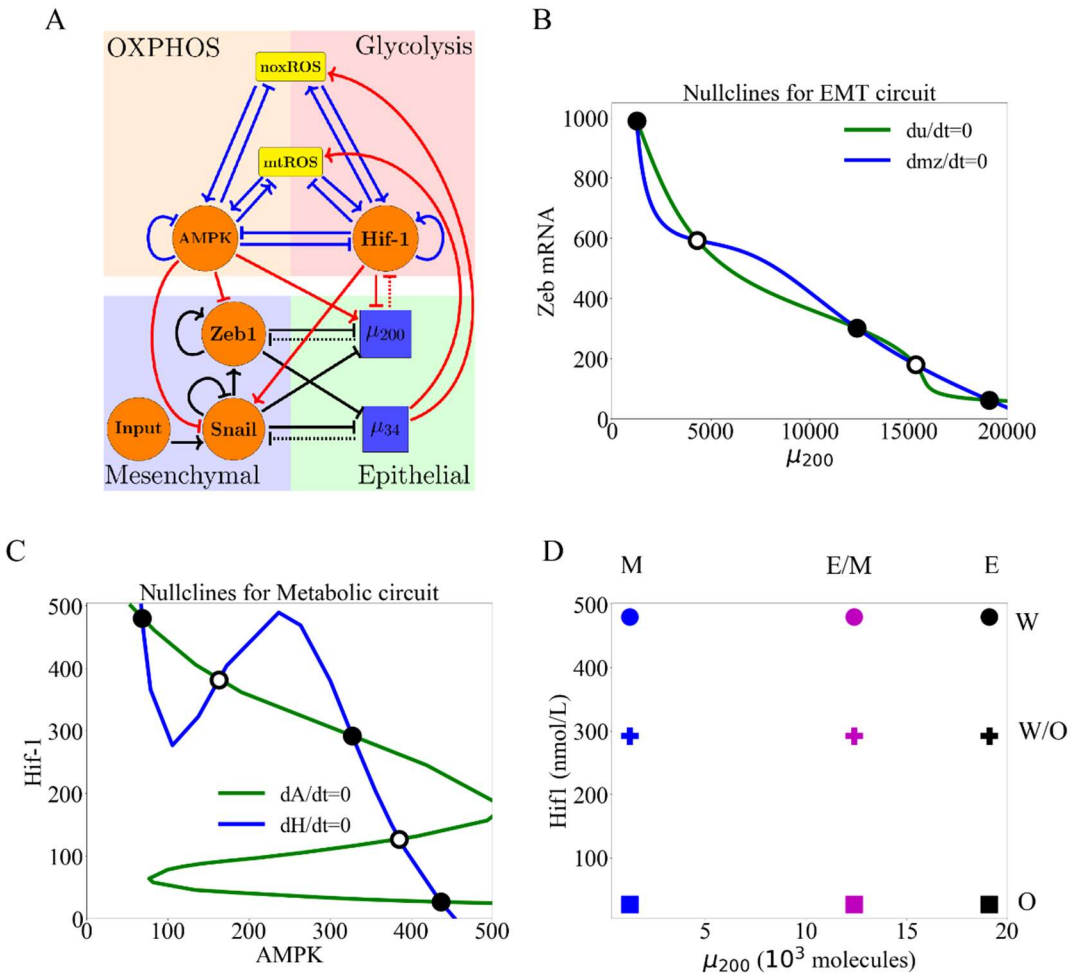

Figure 1. **The coupled EMT/MR circuit results in 9 possible steady states.** With inactive crosstalks all combinations of the steady states of the core EMT and metabolic networks are accessible. **(A)** The network showing the core EMT module (bottom) with regulatory links designated by black, the core metabolic circuit (top) with regulatory links designated by blue, and the crosstalks noted in red. The dashed lines denote miRNA regulation rather than transcriptional regulation. Regulatory links ending in bars represent inhibition while the arrows represent activation links. **(B)** The nullclines of the EMT core network. The system is tristable and the metastable states (high μ_{200}/low Zeb mRNA, low μ_{200}/high ZEB mrNA, and intermediate μ_{200}/ZEB mRNA) correspond to the phenotypes (E, M, E/M). **(C)** The nullclines of the metabolic core network for cancer cells. The system is tristable with metastable states (high AMPK/low HIF-1, low AMPK/high HIF-1, and intermediate AMPK/HIF-1) corresponding to metabolic phenotypes (O, W, W/O). **(D)** The 9 possible phenotypic states when all crosstalks are inactive. The blue, purple, and black markers represent the mesenchymal (M), hybrid epithelial-mesenchymal (E/M), and epithelial (E) steady states, respectively. The circle, cross, and square represent the Warburg (W), hybrid Warburg-OXPHOS (W/O), and OXPHOS (O) metabolic phenotypes, respectively. The coupled E/M-W/O state is therefore represented as a purple cross.

Results

Individual crosstalk links can push the downstream circuit towards a single state: Let us start by making just one cross-link active, caused e.g. by an EMT-related microRNA based regulatory effect. Now, in our model there is a clearly an unaffected upstream subnetwork (EMT, from where the link originates) and a regulated downstream one. (Note that the model ignores any possible dilution of the microRNA due to its action on ROS; see below). When noxROS is upregulated by μ_{34} (Fig. 2A), the EMT network remains unaffected while the hybrid W/O state and the coupled E/M-W/O phenotype are upregulated. As the level of noxROS increases (μ_{34} upregulates noxROS by reducing the degredation), the possible coupled states reduce from nine to six, losing first the E-W state, then the E/M-W, and finally losing the M-W state (Fig. 2B, section S2.4). Analyzing the percent of initial conditions that lead to the various metabolic phenotypes shows that the lost coupled states associated with the Warburg phenotype are pushed towards the W/O phenotype, with little change occurring for the OXPHOS associated states (Fig. 2C).

As there is no feedback to the EMT network, the percentage of E, E/M, and M states are constant; however, the E/M state becomes more likely to be associated with the hybrid W/O metabolic phenotype (Fig. 2D). Analyzing the states coupled with the Warburg phenotype, however, shows the mesenchymal phenotype (M-W) persists longer as the coupling is increased, as expected since it has the lowest μ_{34} level (Fig. 2E). Similar changes emerge via the upregulation of mtROS (Fig. S8); the E-W and E/M-W states are also the first suppressed states. Additionally, upregulating mtROS is also correlated with an upregulation of the E/M-W/O phenotype. Further, activation of mtROS results in a downregulation of the OXPHOS metabolic

phenotype alongside downregulation of the Warburg phenotype. Together, these results suggest ROS is a critical factor in enabling metabolic plasticity as part of tumor progression, and mtROS may play a stronger role than noxROS.

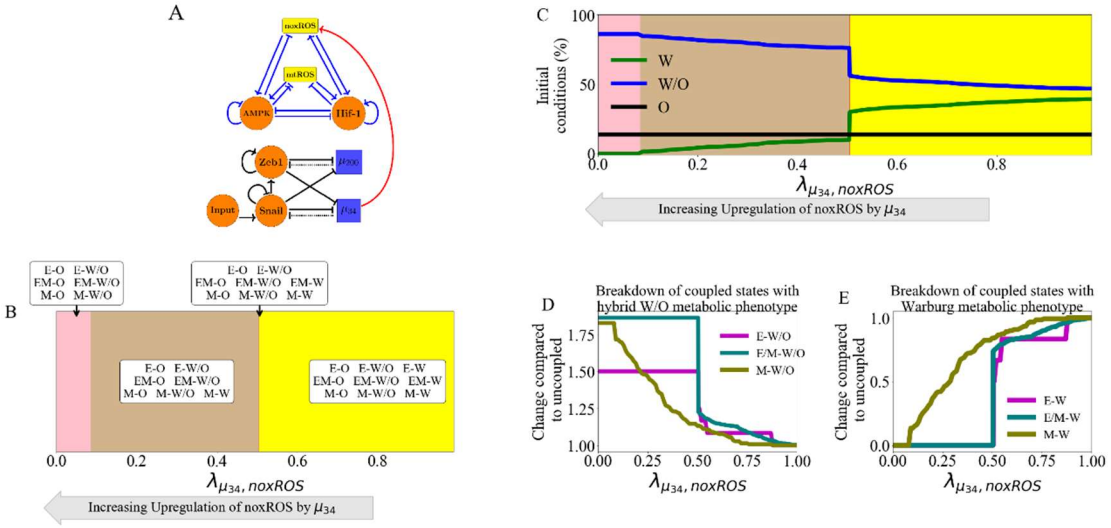

Figure 2. noxROS upregulated by miR-34 results in upregulated W/O phenotype and is associated with upregulated E/M-W/O phenotype. As noxROS is upregulated by miR-34, the number of initial conditions leading to the OXPHOS phenotype is minimally changed, Warburg phenotype is reduced, and W/O phenotype is increased. The EMT network is unchanged but the coupling of metabolic phenotypes to the EMT steady states changes, and the E/M-W/O phenotype is upregulated. **(A)** A diagram of the core EMT circuit (left) and the core metabolic circuit (right) connected by the crosstalk between μ_{34} upregulating noxROS (red link representing transcriptional regulation). **(B)** Of the nine possible coupled states, as noxROS is upregulated by miR-34, there are 4 distinct groupings. All possible couplings of the EMT phenotypes (E, M, and E/M) with both the O and W/O metabolic phenotypes persist for all levels of noxROS upregulation. The coupled states associated with the W metabolic phenotypes, (E-W, E/M-W, and M-W), are lost as the level of noxROS regulation increases for the red, tan, and pink regions, respectively. **(C)** The background colors correspond to the colors representing the possible steady states of (B). The lines represent the total number of initial conditions leading to the W, O, or W/O phenotypes as a function of increasing regulation of noxROS by miR-34. The W/O phenotype (blue) is upregulated, Warburg (green) phenotype is downregulated, and OXPHOS (black) is unchanged. **(D)** Showing the breakdown of the coupled states associated with the W/O phenotype (i.e., E-W/O, M-W/O, and E/M-W/O) compared to the inactive system ($\lambda_{\mu_{34},noxROS} = 1$). The E/M-W/O coupled state is greatly upregulated once $\lambda_{\mu_{34},noxROS} = 0.5$, the M-W/O coupled state is slowly upregulated, and E-W/O is also upregulated. **(E)** Same as (D) but for the coupled states associated with the Warburg phenotype. Once $\lambda_{\mu_{34},noxROS} = 0.5$, both

the E-W and M-W states are fully suppressed. The E/M-W coupled state continues to be downregulated until it is fully suppressed near $\lambda_{\mu_{34},noxROS} = 0.1$.

Regulation of HIF-1 affects both subcircuits: While the previous μ_{34} link only affected the downstream network, the miRNA regulation of HIF-1 by μ_{200} can affect both networks. This arises because of the reduction in the microRNA level caused by this coupling. In our model, miRNA regulation is mathematically represented as three functions (Y_m, Y_u, and L) that modify the degradation of HIF-1 mRNA, the degradation of μ_{200} , and the production of HIF-1. Therefore, while the downstream metabolic network is clearly modulated, the upstream EMT network is also affected via enhanced μ_{200} degradation. These mathematical functions depend on multiple parameters; therefore, we have defined a simplified silencing function (detail of silencing function $P_H(\mu)$ in section S2.5) that groups subsets of the results based on the parameters and the value of μ_{200}. Note that as we include increased silencing, the first thing which occurs is the restriction of the EMT state; fairly close to $P_H(\mu) = 1$, the only EMT state allowed is M. When we enter this region, all the metabolic phenotypes are allowed. As the silencing increases, the mixed W/O and W states are suppressed sequentially. As HIF-1 decreases and we transition to the O state, the enhanced degradation of μ_{200} diminishes and the EMT system loses the mesenchymal state. When HIF-1 mRNA is fully silenced, only the E-O and E/M-O coupled states remain (Fig. 3). Since the E/M state does not reappear until after the metabolic system has fully transitioned to O, the hybrid E/M-W/O state is suppressed for all values of μ_{200} silencing HIF-1 mRNA. These results suggest μ_{200} overexpression could destabilize the E/M-W/O phenotype.

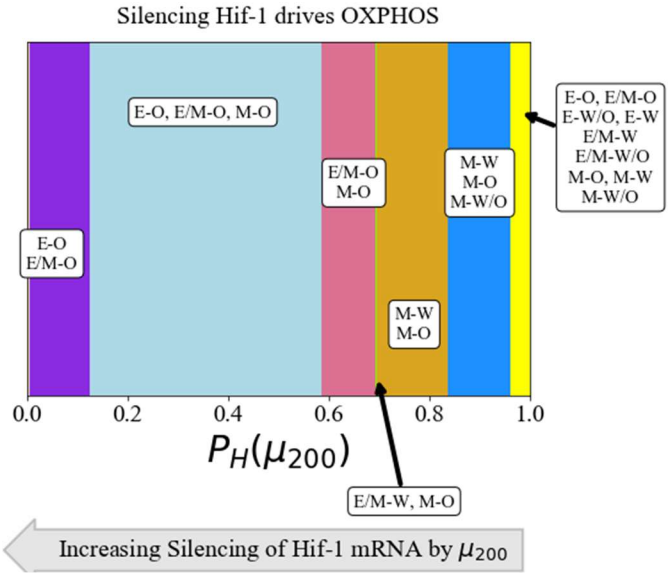

Figure 3. The coupled phenotypes associated with increased silencing of the HIF-1 mRNA by μ_{200}. Both the EMT and metabolic networks are affected by the miRNA regulation of HIF-1, and the E/M-W/O phenotype is suppressed if any fraction of silencing occurs. At minimal silencing ($P_H(\mu_{200})$ near 1) only the coupled states with mesenchymal phenotypes are accessible (M-W, M-O, and M-W/O). Then as silencing increases the mixed metabolic phenotype is lost, then the M-W state becomes E/M-W, and after that only the coupled states with OXPHOS metabolic phenotype are accessible. At complete silencing of the HIF-1 mRNA only the E-O and E/M-O states are accessible.

Inclusion of all miRNAs of the EMT network can stabilize the W/O metabolic phenotype:

We next wish to determine how including links emanating from both miRNAs of the EMT network can synergistically drive metabolic reprogramming, and specifically enhance the chances of being in the E/M-W/O state. As mentioned previously, upregulated ROS leads to an increased W/O phenotype (Fig. S8). If both noxROS and mtROS are upregulated by μ_{34} the E/M-W/O state is further upregulated (Fig. S15). While upregulation of ROS causes an increase in the hybrid E/M-W/O, we showed above that μ_{200} silencing HIF-1 mRNA suppresses the hybrid E/M-W/O state; therefore, some suppression of the hybrid E/M-W/O state is expected when μ_{200} and μ_{34} regulate HIF-1 and ROS, respectively. Interestingly, the hybrid E/M-W/O

state can be fully suppressed when μ_{200} downregulates HIF-1 and μ_{34}upregulates noxROS, but only partially suppressed when μ_{200} downregulates HIF-1 and μ_{34} upregulates mtROS (Fig. S16). These results suggest the type of ROS present can affect the existence of the E/M-W/O state.

The hybrid E/M-W/O state is stabilized if mtROS is upregulated, but noxROS upregulation has minimal effect on the hybrid E/M-W/O state. Strikingly, if all three miRNA crosstalks are active (μ_{200} silencing HIF-1 mRNA and μ_{34} upregulating noxROS and mtROS, Fig. 4A) the E/M-W/O coupled state may be suppressed even if the W/O state is present (Fig. 4B). Further, the E/M-W/O phenotype is present for all values of noxROS upregulation but is only present at high values of mtROS upregulation (Fig. 4B). Analyzing the coupled state phases shows the E/M-W/O state is suppressed when mtROS is only slightly upregulated (Fig. 4C). Further, the epithelial and E/M states are associated with the OXPHOS phenotype when mtROS levels are slightly upregulated. Interestingly, the mesenchymal state is coupled with O and W/O metabolic phenotypes while the E and E/M states are only coupled to the W/O phenotype when mtROS is fully upregulated. Additionally, depending on the initial conditions, if noxROS is maximally upregulated, mtROS is upregulated, and HIF-1 is partially silenced by μ_{200} the system can access the hybrid E/M-W/O state (Fig 4D). Also, while mtROS must be upregulated for the system to access the E/M-W/O state, the hybrid state is accessible for all levels of noxROS upregulation (SI Fig S17). The difference in the effect of noxROS and mtROS seems to result from the frustrated regulation of mtROS by HIF-1 and μ_{34}. Therefore, feedback links between mtROS, HIF-1, μ_{34}, and μ_{200}may control the appearance of the E/M-W/O state.

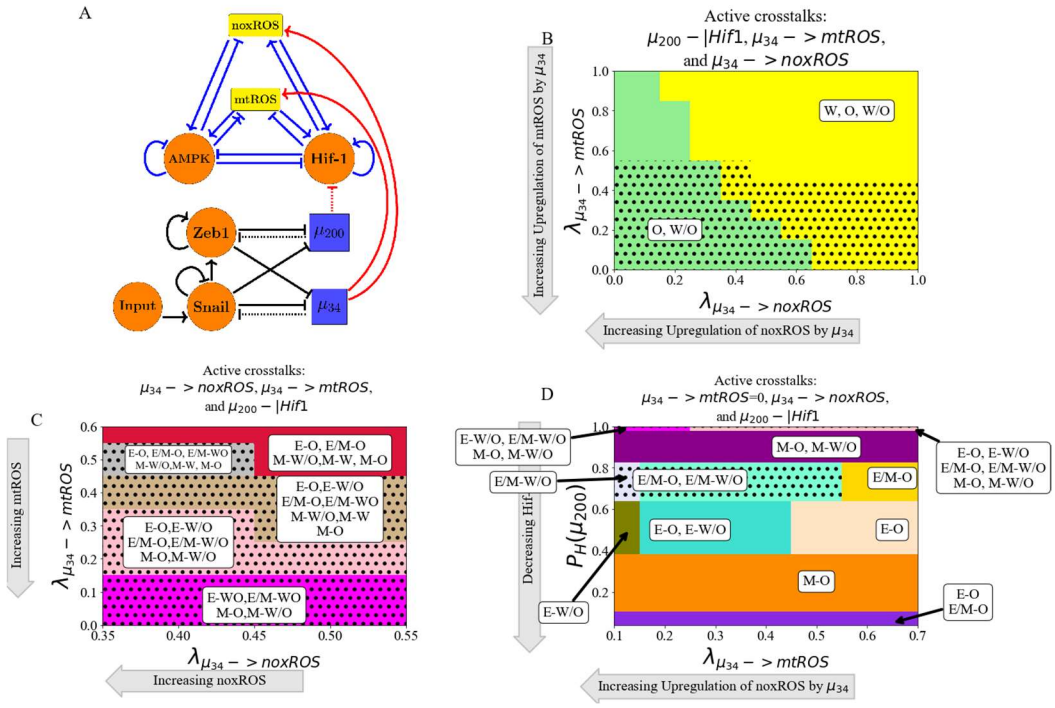

Figure 4. miRNA of the EMT regulatory network can upregulate the W/O phenotype. When all three crosstalks from the EMT network (μ_{200}-|HIF-1, μ_{34}-> mtROS, and μ_{34}->noxROS) are active the E/M-W/O state can be upregulated. The E/M-W/O state is accessible when mtROS is high and at intermediate silencing of HIF-1. The level of noxROS seems to have minimal effect. This suggests the μ_{34}/μ_{200}/HIF-1/mtROS axis plays a significant role in stabilizing the hybrid E/M-W/O state. **(A)** The coupled metabolic (top) and EMT (bottom) regulatory network with all EMT driven regulatory links active (μ_{34} upregulating mtROS, μ_{34} upregulating noxROS, and μ_{200} silencing HIF-1). **(B)** The phase plane corresponding to all EMT driven regulatory links (network pictured in A). The regulation of HIF-1 by μ_{200} in this phase plane corresponds to the rightmost, blue region of Fig. 3 where all metabolic phenotypes are possible. As noxROS is upregulated (right to left), the Warburg metabolic phenotype is suppressed. However, as the level of mtROS increases (top to bottom), the black dotted region appears showing the existence of the E/M-W/O coupled state, suggesting mtROS may have a stronger effect on the E/M-W/O phenotype than noxROS. **(C)** The coupled states when only EMT driven crosstalks are active (μ_{200} downregulating HIF-1 and μ_{34} upregulating mtROS and noxROS). The E/M-W/O state exists when mtROS is upregulated. **(D)** At maximum upregulation of noxROS ($\lambda_{\mu_{34}->noxROS}$=0), as mtROS increases (x-axis) and HIF-1 is silenced (y-axis) there are regions where the E/M-W/O state is possible (black dotted regions).

Metabolic reprogramming can drive EMT: We next turn to a consideration of information flowing in the other direction, from metabolism to EMT. To elucidate the way in which metabolic reprogramming can drive EMT, we determined the effect of each metabolism-driven

crosstalk on the coupled states. First, we analyzed the links in which HIF-1 upregulates SNAIL (Fig. 5A and S9) or inhibits μ_{200} (Fig. S10). As expected, both HIF-1 driven links push the system towards the mesenchymal state. Further, both the epithelial and hybrid E/M states are most associated with the OXPHOS metabolic state (with smaller HIF-1) while the mesenchymal state is initially associated with the Warburg state. The correlation between the epithelial-OXPHOS and mesenchymal-Warburg states is assumed in much of the literature[30]. Similarly, modulating the external input to SNAIL can alter the presence of the E/M state and increasing this input pushes the system towards mesenchymal (see Fig. S11). Opposite to the HIF-1 results, AMPK upregulating μ_{200} pushes the EMT network to adopt an epithelial phenotype and suppresses the E/M state before suppressing the mesenchymal state (Fig. 5B and S12). Similarly, AMPK downregulation of ZEB and/or SNAIL has a corresponding effect on the expression of the E/M state and the systems saturates near fully mesenchymal (Fig. S13 and S14). Additionally, if AMPK is regulating the EMT circuit, the epithelial and mesenchymal states are still most associated with the OXPHOS and Warburg metabolic phenotypes, respectively. However, the E/M state for AMPK driven crosstalk is associated with the Warburg state. This is in direct contract to HIF-1 driven crosstalk in which the E/M state is coupled with OXPHOS metabolism. The dependence of the coupled metabolic phenotype on the regulator of the crosstalk link , suggests neither OXPHOS nor Warburg metabolism is automatically associated with the E/M phenotype and that this state has a relatively flexible metabolism.

The sets of coupled phenotypes present can be compared between models with different active crosstalk links, as the regulation is increased. Comparing noxROS and mtROS upregulation, the E-W and E/M-W coupled states are the first suppressed. Additionally, both crosstalks upregulate the E/M-W/O state, although when mtROS is upregulated only the

mesenchymal phenotype is coupled with OXPHOS metabolism. The phases are also very similar whether HIF-1 inhibits μ_{200} or upregulates Snail. However, the E/M-W/O state does persist longer when HIF-1 inhibits μ_{200} (Fig. S9 and S10). Lastly, the AMPK driven crosstalks are initially very similar. In fact, the phases are nearly identical when AMPK inhibits ZEB or SNAIL (Fig. S13 and S14). However, AMPK upregulating μ_{200} has slightly different phases before saturating at epithelial (Fig. S12). These similarities between crosstalk effects suggests a degree of consistency between the different ways that EMT can drive metabolic reprogramming, or vice versa.

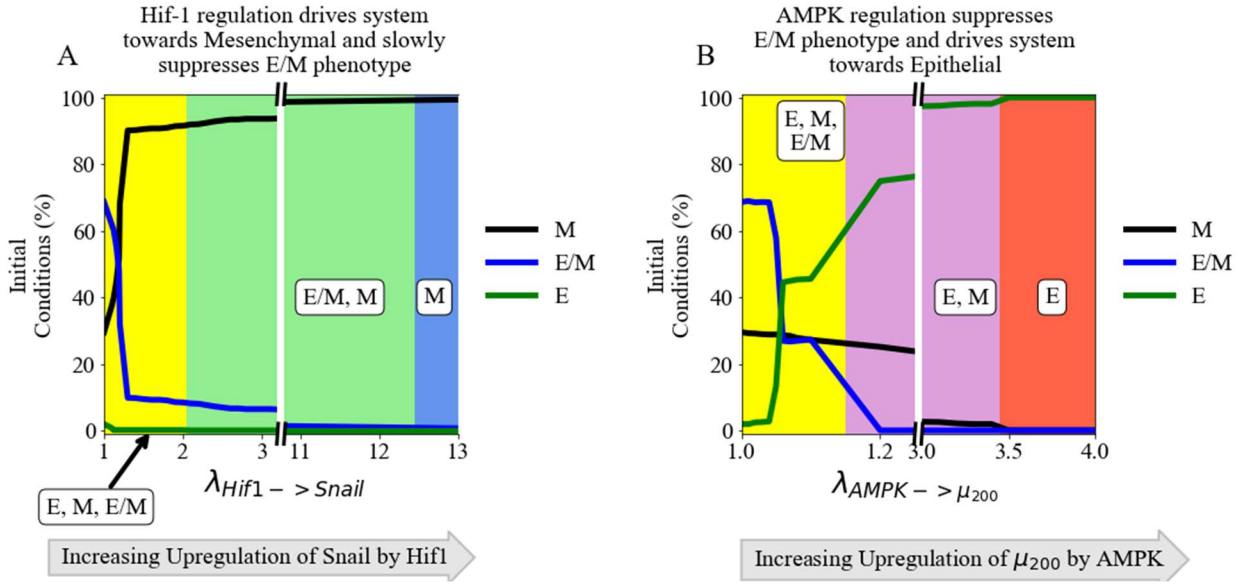

Figure 5. The role of metabolic driving of EMT. HIF-1 controlled crosstalks drive the EMT circuit towards the mesenchymal state, while AMPK controlled crosstalks drive the EMT network towards the epithelial state. Neither type of crosstalk can stabilize the E/M state, but the E/M state persists longer for HIF-1 controlled crosstalks. **(A)** The number of initial conditions leading to an E/M, M, or E phenotype as HIF-1 upregulates SNAIL. The hybrid E/M phenotype is suppressed quickly as the system is driven towards mesenchymal. **(B)** Similar to (A) but for AMPK upregulating μ_{200} and driving the system towards epithelial. The E/M state persists longer for HIF-1 regulation than for that based on AMPK.

TFs of the metabolic network can stabilize the E/M metabolic phenotype: There are two distinct events at play when the metabolic network regulates the EMT circuit. AMPK regulation quickly suppresses the E/M phenotype and pushes the system towards the Epithelial state whereas HIF-1 regulation can allow the system to maintain the E/M phenotype for a range of strengths while ultimately pushing the system towards mesenchymal (Fig. 5A and 5B). As AMPK and HIF-1 push the system towards opposite states, having active links emanating from both should push the circuit towards a hybrid state. That is exactly what happens for any combination of the three AMPK crosstalks and two HIF-1 crosstalks, although the exact values of where the E/M-W/O state exists depends in detail on the type of regulation (Fig. S18). Additionally, if AMPK and HIF-1 target different EMT TFs, the E/M-W/O state may exist in more parameter regions than if they target the same TF (Fig. S18), suggesting multiple crosstalks must be active and multiple gene regulators must be targeted to stabilize the E/M-W/O state. If all crosstalks involving AMPK and HIF-1 regulating the EMT circuit are active (Fig. 6A) then there are significant regions in which the E/M state exists (Fig. 6B). However, when analyzing the system for the existence of the E/M-W/O phenotype, it only exists in a small region when μ_{200} is minimally upregulated. Moreover, HIF-1 driven crosstalks are able to maintain the E/M phenotype longer than AMPK driven crosstalks suggesting, the reduced regions of E/M-W/O existence is likely due to the suppression of the E/M state by AMPK regulated crosstalks, as mentioned above (see Fig. S12-S14). This suggests HIF-1 driven crosstalk is more strongly correlated with the E/M state than AMPK driven crosstalk, in agreement with a recent study based on publicly available expression data[67].

To stabilize the E/M state, both AMPK and HIF-1 crosstalk are necessary, and if all EMT regulating crosstalks are active then there are regions where the E/M-W/O state exists. Additionally, the epithelial state is typically coupled to OXPHOS metabolism (E-O), the mesenchymal state is associated with the Warburg metabolic phenotype (M-W), and when the E/M state is present it is typically associated with the hybrid W/O metabolic phenotype (Fig. 6C). In fact, for any system, if there are only three coupled states available and each has a distinct phenotype of the EMT and metabolic networks, then the only possible set of states is E-O, M-W, and E/M-W/O. This behavior represents the full coordination of EMT and metabolism and suggests that cells in the primary tumor prefer to utilize OXPHOS while clusters of migrating cells utilize a combination of aerobic glycolysis and OXPHOS.

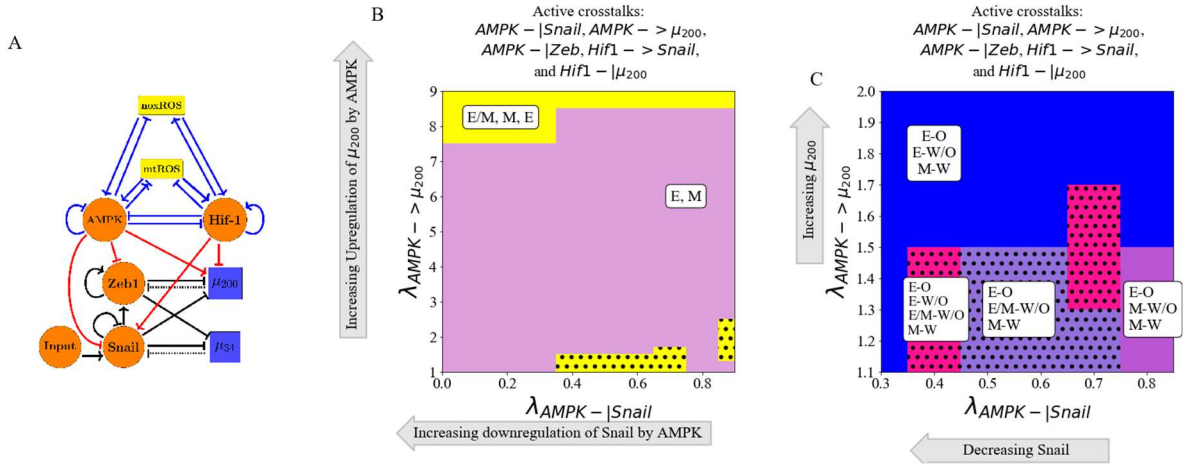

Figure 6. AMPK and HIF-1 cooperate to upregulate the hybrid E/M state. When all HIF-1 and AMPK controlled crosstalks are active (HIF1->Snail, HIF1-|μ_{200}, AMPK-|Snail, AMPK-|Zeb, AMPK-> μ_{200}) the E/M-W/O state can be stabilized. HIF-1 driving the network to mesenchymal and AMPK driving the system towards the epithelial state results in HIF-1 and AMPK cooperatively stabilizing the E/M state. Once stabilized, the E/M state is coupled with the W/O state (i.e., stabilizing the hybrid E/M-W/O state). **(A)** The network showing metabolism driven crosstalks. ZEB is inhibited by AMPK, SNAIL is upregulated by HIF-1 while being downregulated by AMPK, and μ_{200} is upregulated by AMPK while being inhibited by HIF-1. **(B)** The phases plane of potential EMT phenotypes when all metabolic driven crosstalks are active. The E/M phenotype is only accessible when $\lambda_{AMPK-|\mu200}$ is near 1 or very high (i.e., at the extremes of regulation). **(C)** The coupled states when only TFs and miRNAs of the EMT circuit are regulated by TFs of the metabolic circuit (AMPK-|SNAIL, AMPK-|ZEB, AMPK->μ_{200},

HIF-1 -|μ_{200}, HIF-1 -> SNAIL). The results suggest a correlation between the E, E/M, and M phenotypes to the O, W/O, and W metabolic phenotypes.

The Hybrid E/M-W/O phenotype: Recently, it has been suggested that the most aggressive cancers phenotypes are characterized by the hybrid E/M state and mixed metabolism, enabling a high degree of plasticity and thereby enabling metastatic spread and drug resistance[30]. Therefore, it is now useful to focus our discussion onto how the crosstalk in both directions specifically affects the presence of the E/M-W/O state and the possibility that it could be the only possible coupled state for some set of parameters. From our analysis of activating individual crosstalks, we deduce that a metabolic driven crosstalk and two competing EMT driven crosstalks would be minimally necessary to fully stabilize the E/M-W/O state and suppress all other coupled states.

In detail, the hybrid E/M-W/O state can be stabilized when AMPK downregulates SNAIL, HIF-1 downregulates μ_{200}, and μ_{34} upregulates mtROS. The E/M-W/O phenotype exists in much of the space and is increased in prevalence when the downregulation of SNAIL by AMPK has pushed the system to be in the nearly mesenchymal regime ($\lambda_{\text{AMPK-| SNAIL}}$=0.2), mtROS is increased, and μ_{200} levels have decreased (Fig 7A and S19A). Further, instead of HIF-1 downregulating μ_{200}, the Input to SNAIL can be increased, causing the E/M-W/O state to become even more dominant (Fig. 7B and S19B). While, the E/M-W/O state was stabilized in both cases, neither was able to fully stabilize the E/M-W/O state and suppress all other states.

It is possible to suppress all states except the hybrid E/M-W/O state with just three regulatory links; HIF-1 inhibiting μ_{200}, μ_{34} upregulating mtROS, and modulating the Input to SNAIL (Fig. 7C and S19C). In fact, no other combination consisting of only three regulatory

links seems to suppress all states except the E/M-W/O state, even if a crosstalk is replaced by modulating the Input to SNAIL. Additionally, this region which only includes the E/M-W/O state persists even if all remaining crosstalks are activated (Fig. 7D and S19D).

Looking at the proximal phases next to the one with just E/M-W/O suggests that stabilization of the E/M-W/O state is driven by mutual activation of metabolic reprogramming and EMT. When the E/M-W/O state is the only one available (Fig. 7C and 7D), the nearby phases are the same whether only three crosstalks or all crosstalks are active (E-O and E-W/O), suggesting there is a progression that must be followed to generate the E/M-W/O state. Further, if the E/M-W/O state is only increased in importance but not the only allowed state (Fig. 7A and 7B), the surrounding phases include mesenchymal coupled states (M-O, M-W/O, and M-W) as well as (E-O and E-W/O). This suggests that first metabolic reprogramming occurs (E-W/O) followed by a partial EMT (E/M-W/O). Consequently, this suggests the system can only fully transition to E/M-W/O if the cells are initially in the E-O state, but the population of the E/M-W/O state can be enhanced if the cells are in other states at the start of the transition. Additionally, the persistence of the E/M-W/O state suggests there might be other combinations of crosstalks that generate phases where only the E/M-W/O state is possible, although it is outside the scope of this manuscript to find all possible combinations of crosstalks that can suppress all states except the hybrid E/M-W/O coupled state. However, based on these results, we would expect HIF-1 suppressing μ_{200} and μ_{34} upregulating mtROS to be prominent among all such combinations.

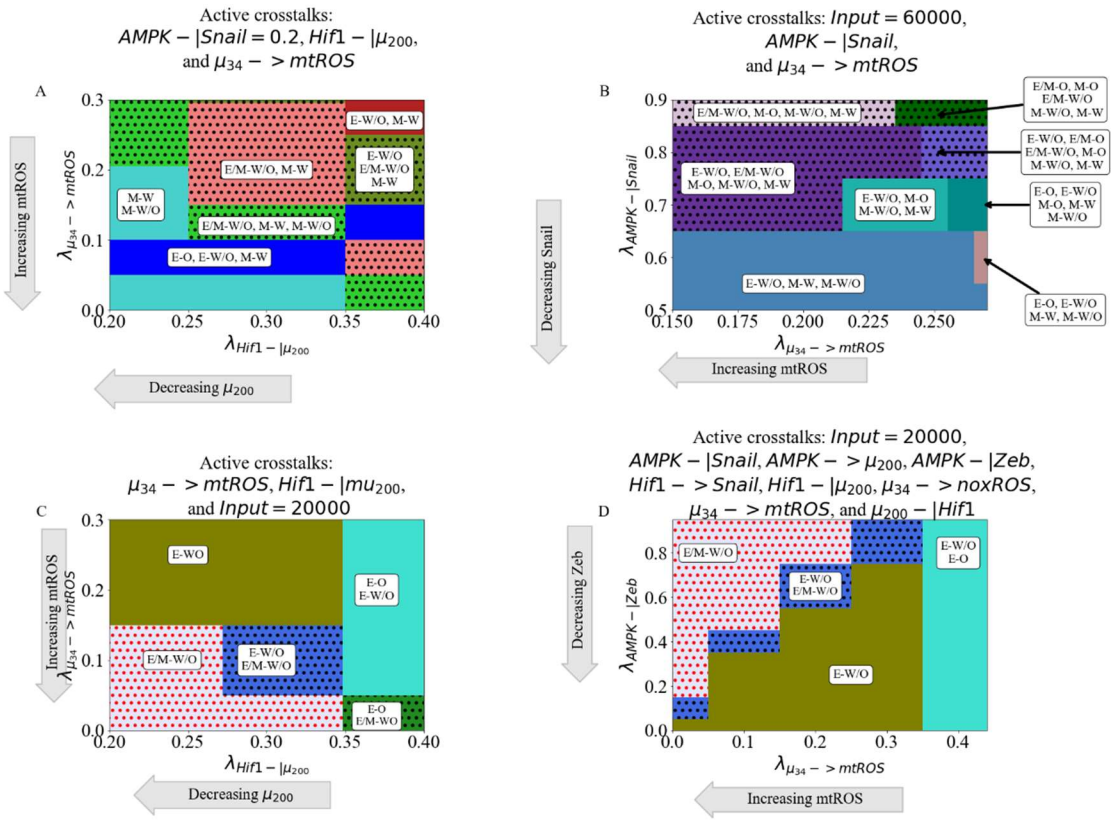

Figure 7. The EMT and metabolic regulatory networks crosstalks can drive the system to the hybrid E/M-W/O coupled state. Minimally, three links (one effecting the metabolic network and two controlling the EMT network) are necessary to suppress all coupled states except the E/M-W/O state. Many combinations of crosstalks can upregulate the E/M-W/O state, but to stabilize only the E/M-W/O state it seems that mtROS must be upregulated, μ_{200} must be inhibited and the Input to SNAIL should be decreased. Additionally, based on the states surrounding the E/M-W/O phase (E-O leading to E-W/O and stabilizing at E/M-W/O), metabolic reprogramming drives EMT. **(A)** The coupled states when the Input=60000, AMPK downregulates SNAIL, and μ_{34} upregulates mtROS. The E/M-W/O state is upregulated when mtROS levels are increased. **(B)** The phase plane when $\lambda_{\text{AMPK-| SNAIL}}$=0.2, HIF-1 inhibits μ_{200} production, and μ_{34} upregulates mtROS. The E/M-W/O state is upregulated for some regions. **(C)** When crosstalks mutually drive EMT and metabolic reprogramming, there are parameter regions in which the only possible coupled state is the E/M-W/O state. **(D)** When all crosstalks are active there are regions where only the E/M-W/O state exists. Similar sets of coupled states in (C) and (D) suggest a preferential pathway to drive the system towards the hybrid E/M-W/O coupled state.

Normal cells can exhibit hybrid properties when crosstalks introduced: We have confirmed that the E/M and W/O states are often connected, the population in the E/M-W/O state can be

expanded depending on the relative strength of various links, and there are parameter sets with only the hybrid E/M-W/O state available and all other coupled states suppressed. However, these results were obtained for a network model in the parameter regime typical of cancer cells (i.e., tristable circuits with a hybrid intermediate state). Under normal physiological conditions, we expect that most cells will be restricted to a binary choice of E versus M and W versus O[68]. To determine whether under these conditions EMT can drive metabolic reprogramming, and vice versa, we modify the network to be in the parameter regime of normal cells (i.e., bistable systems with no hybrid state). A few key parameters were modified to affect SNAIL regulating μ_{200}, SNAIL regulating ZEB, HIF-1 degradation, HIF-1 mRNA degradation, and the competitive regulation of mtROS by AMPK and HIF-1 (see Section S1.5 for parameters). We confirmed both the EMT and metabolic networks are independently bistable when the crossstalks are inactive, by calculating the nullclines for the system (Fig. S20), and ensured the solutions from the initial conditions were evenly divided between the steady states (Fig. S21-S22). We can then proceed to determine the consequences if EMT drives metabolic reprogramming, metabolic reprogramming drives EMT, or both .

As already mentioned, the EMT network can drive metabolic reprogramming via microRNA dependent links. We first kept the EMT circuit as a tristable network but changed the parameters of the metabolic circuit to reflect normal cells (i.e., no hybrid W/O state in the inactive network). Then we analyzed the coupled phenotypes when either μ_{34} upregulates mtROS, μ_{200} downregulates HIF-1, or μ_{34} upregulates noxROS. The metabolic circuit becomes tristable (generates the mixed W/O phenotype) at high levels of mtROS upregulation (Fig. 8A). Additionally, when μ_{34} activates mtROS it can even upregulate the E/M-W/O state so that all E/M phenotypes become coupled with the hybrid metabolic W/O phenotype. However, the

system remains bistable and the hybrid metabolic phenotype is not generated if only noxROS is upregulated or μ_{200} is downregulated (Fig. S23). Interestingly, minimal change occurs for the coupled phenotypes when μ_{200} silences HIF-1 mRNA. Furthermore, the upregulation of noxROS in the bistable circuit causes an increase in OXPHOS metabolism, in contrast to an increase of the hybrid W/O state in the tristable circuit. This suggests, noxROS may play a context dependent role, unlike mtROS which can stabilize the E/M-W/O phenotype.

Metabolic reprogramming can drive EMT if HIF-1 controlled crosstalks are active. Opposite to the above protocol, we kept the metabolic circuit as a tristable circuit and modifed the EMT network to be bistable (i.e., no hybrid E/M state in the inactive network). Then we investigated the effects as a single crosstalk is turned on. When HIF-1 inhibits μ_{200}, the system is able to quickly generate the E/M-W/O state before it is once again suppressed (Fig. 8B). However, the E/M phenotype persists but is coupled to the OXPHOS metabolic phenotype (E/M-O). Additionally, when HIF-1 upregulates SNAIL the E/M-W/O state is only generated at low levels of SNAIL upregulation (Fig. S24). Furthermore, both systems saturate near mesenchymal while maintain the hybrid E/M phenotype (E/M-O, M-W, M-O, M-W/O). This suggests the master regulator of metabolic reprogramming, HIF-1, can drive normal cells towards the E/M phenotype which would otherwise be inaccessible. Conversely, an individual AMPK driven crosstalk is unable to generate the hybrid E/M state and saturates near the fully epithelial phase (Fig. S24), as seen in the tristable circuit. Additionally, as with the tristable networks, the hybrid E/M-W/O state can be stabilized by two competing crosstalks, such as AMPK upregulating SNAIL and HIF-1 downregulating μ_{200} (Fig. S25). These results suggest HIF-1 can strongly affect and drive EMT into a hybrid state while AMPK can only help stabilize the E/M-W/O state if it is already present.

When both networks are in the parameter regime of normal cells (i.e., no E/M or W/O states are present with inactive crosstalks), metabolic reprogramming drives EMT. Recall that for the coupled tristable circuits, the simplest set of crosstalks with a parameter region that suppressed all coupled states except the E/M-W/O state consisted of three regulatory links; HIF-1 inhibiting μ_{200}, μ_{34} upregulating mtROS, and modulating the Input to SNAIL. When these same links are active for the bistable circuit, the results are qualitatively very similar to the tristable circuit results (Fig. 8C and S26 compared to Fig. 7C). The E/M state is only possible near full inhibition of μ_{200} and the W/O state is possible when mtROS is greatly upregulated. Further, the system must be near maximum regulation (i.e. both fold changes must be close to zero) to generate the region where only the hybrid E/M-W/O coupled state is possible. Additionally, the nearby phases correspond to the phases of the tristable circuit (E-O and E-W/O), further supporting the existence of a progression that must be followed to stabilize the E/M-W/O state.

Overall, we can identify the following scenario. Metabolic reprogramming drives EMT starting with an epithelial cell using OXPHOS metabolism. The transition then proceeds from E-O to E-W/O to E/M-W/O. In other words, metabolism must first be reprogrammed to hybrid W/O which then drives the initiation of EMT and stabilizes the hybrid E/M state.

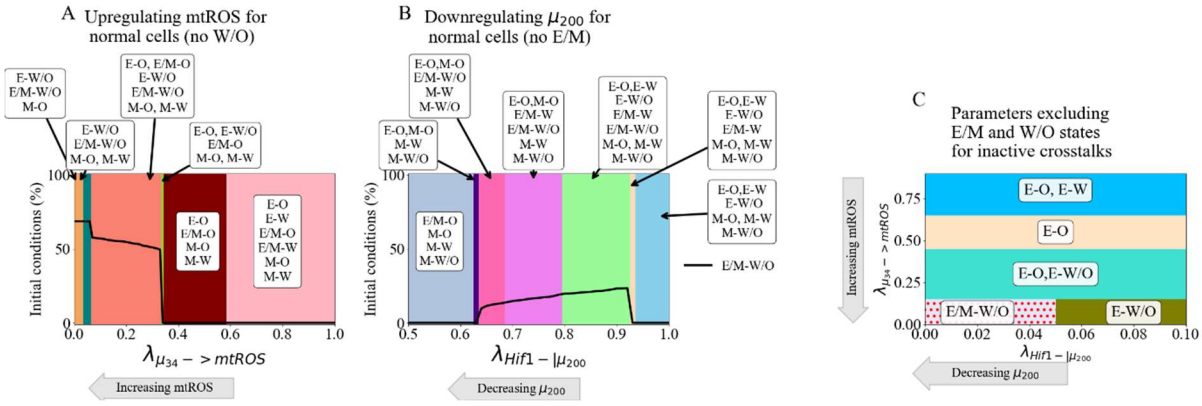

Figure 8. Parameter ranges which exclude the possibility of the hybrid state can be modulated by crosstalk to generate the hybrid state. The activation of a single crosstalk (μ_{34}-> mtROS, HIF1 -> SNAIL, or HIF1 -|μ_{200}) can generate the hybrid state of the downstream network (W/O, E/M, or E/M), respectively. If the metabolic network is bistable (W or O phenotypes) and the EMT network is tristable (E, E/M, or M phenotypes), μ_{34} upregulating mtROS can generate the W/O state and upregulate the E/M-W/O state. Conversely, if the EMT network is bistable (E or M) and the metabolic network is tristable (W, O, or W/O), a HIF-1 controlled crosstalk can briefly generate the E/M state and stabilize the E/M-W/O state. If both networks are bistable, the same three links as the tristable case (μ_{34}-> mtROS, HIF1-|μ_{200} and reducing Input to SNAIL) generates the E/M-W/O state and suppresses all other coupled states. **(A)** Our model using parameters that remove the hybrid W/O metabolic state from the steady state possibilities when the crosstalk is inactive ($\lambda_{\mu_{34}->mtR} = 1.$). Initially, only the OXPHOS and Warburg metabolic states can be accessed with an increase in the percent of OXPHOS steady states and decrease in Warburg phenotypes. Once $\lambda_{\mu 34} = 0.35$, there is a sharp change with the hybrid W/O phenotype becoming the most often occupied phenotype. **(B)** Our model using parameters that remove the hybrid E/M phenotype from the accessible states when the crosstalks are inactive. As the inhibition increases ($\lambda_{Hif\ |\mu_{200}}$ goes towards zero), the system goes from only the E and M states available to regions in which the E/M phenotype is accessible. **(C)** Combining the models from (A) and (B), we generate a model which only has 4 possible coupled states if the crosstalks are inactive (E-O, E-W, M-O, and M-W). At maximum upregulation of mtROS and downregulation of μ_{200}, the E/M-W/O state is the only one accessible, similar to the model with parameters always allowing access to the E/M-W/O state (Fig. 7C).

PSFs can stabilize the hybrid E/M-W/O state: Lastly, we investigate the effects of the crosstalks when the system is already stabilized in the E/M-W/O hybrid state. The PSFs GRHL2 and OVOL are known to stabilize the hybrid E/M state[14,46]. Also, since GRHL2 upregulates ROS in a manner similar to μ_{34}[69], GRHL2 should stabilize the W/O phenotype. Therefore, we modified the original tristable network to include these PSFs (Fig. 9A, parameters and modified

equations of the PSF stabilized network are in Section S1.6). When the crosstalks are inactive, we find the PSF stabilized network can either be in the E/M-W/O or E/M-O state, and more than 90% of initial conditions lead to the hybrid E/M-W/O state (Fig. S27).

When a single crosstalk is active in the PSF coupled network, the behavior is as expected, with the E/M-W/O state persisting for more parameter values than in the original tristable coupled network. For instance, the hybrid E/M-W/O state is stabilized at all values of the fold change for AMPK downregulating SNAIL, AMPK upregulation μ_{200}, and μ_{34} upregulating noxROS (see Fig. S28). However, when HIF-1 downregulates μ_{200} or HIF-1 upregulates SNAIL, the E/M-W/O state is only stabilized for some values of the fold change, but the E/M-W/O is present for more values when PSFs stabilize the circuit compared to the original tristable network (Fig. S28). These results confirm the PSFs increase the stability of the E/M-W/O state, even when EMT-metabolism crosstalks are active.

When multiple crosstalks are active, the stability of the E/M-W/O state persists. If two competing crosstalks acting on the EMT circuit are active (i.e., one HIF-1 and one AMPK driven regulation active), then the E/M-W/O state is possible for most of the parameter space (Fig. 9B). The regulatory crosstalks controlled by HIF-1 seem to have a stronger affect than the AMPK crosstalks and can push the system towards mesenchymal, as shown by the presence of the M-W/O state as μ_{200} is inhibited by HIF-1. This corresponds with results from the tristable and bistable coupled networks where AMPK upregulating μ_{200} seems to have a weaker effect, specifically on the stability of the E/M-W/O state, than HIF-1 downregulating μ_{200}. Lastly, we activate the three crosstalks that were shown in the tristable and bistable networks to suppress all states except the E/M-W/O state; μ_{34} upregulates mtROS, HIF-1 downregulates μ_{200}, and the Input to SNAIL is modulated. Once again, there is a phase where only the E/M-W/O state exists.

Furthermore, this phase exists in a far larger region when stabilized by the PSFs than for the corresponding tristable or bistable coupled network (Fig. 9C and S29). Specifically, the light red region at the bottom left corner of Fig. 9D, shows the parameter space where the E/M-W/O state is the only one available for the tristable network at this level of Input to SNAIL. The large red region surrounding it is the additional parameter space the E/M-W/O state is stabilized when the PSFs are coupled with the network. Further, the states in the phases surrounding the region of E/M-W/O stability are the same as the bistable networks (E-W/O and E-O), and also correspond to those of the tristable network. Thus, incorporating the PSFs – GRHL2 and OVOL – can increase the stability of the E/M-W/O state and the results here agree with our previous finding of mutual activation between the EMT and metabolic networks.

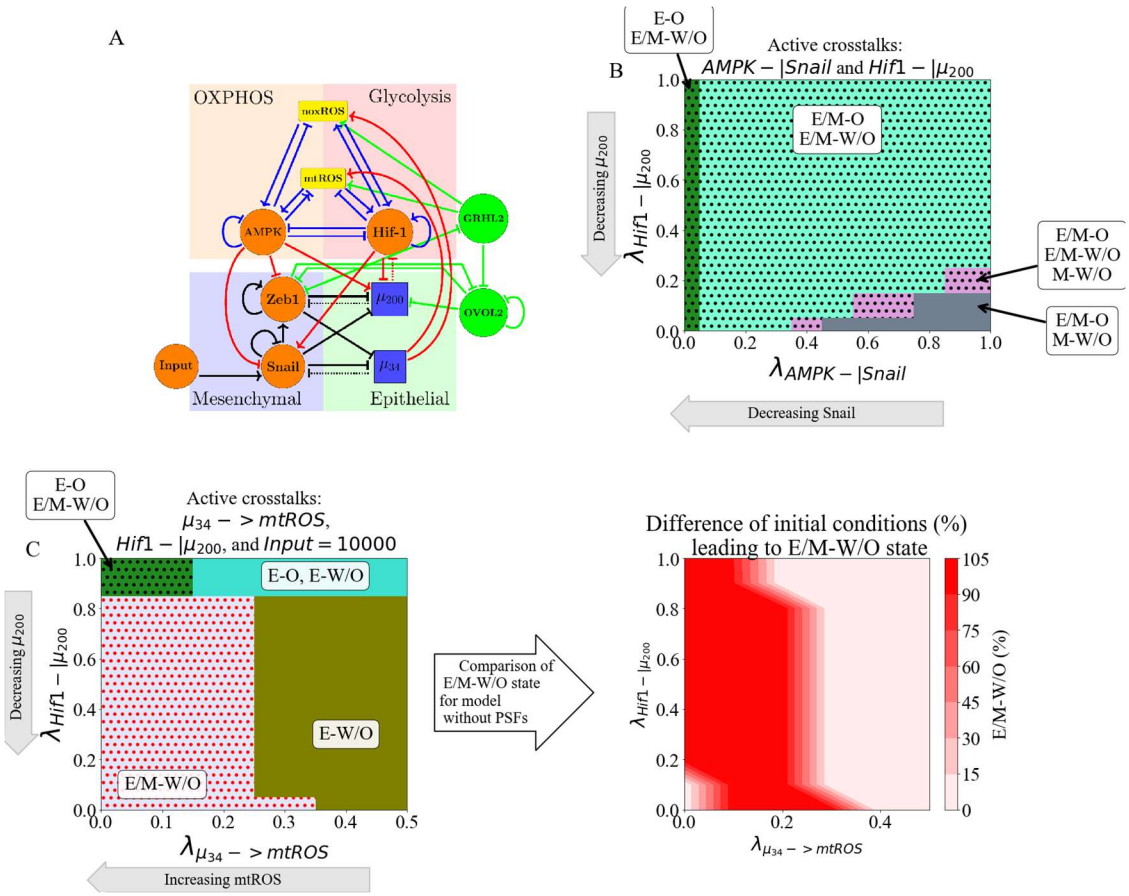

Figure 9. PSFs stabilizing E/M state can increase parameters spaces of E/M-W/O states. Including the PSFs GRHL2 and OVOL2 further stabilizes the E/M-W/O state. Once again, the three links (μ_{34}-> mtROS, HIF1-$|\mu_{200}$, and reducing Input to SNAIL) suppresses all states except the E/M-W/O state and increases the parameter regime of the phase. **(A)** The modified network to include GRHL2 and OVOL2. **(B)** The coupled E/M-W/O state is present in more of the space due to the PSFs stabilizing the E/M state even when AMPK downregulates SNAIL and HIF-1downregulates μ_{200}. **(C)** The phase space when the Input to SNAIL is set to 10K, μ_{34} is upregulating mtROS, and HIF-1 is downregulating μ_{200}. There is a larger region where the E/M-W/O state is the only possible coupled state compared to the original model. **(D)** The difference in the percent of initial conditions between (C) and the original model when the Input to SNAIL is 10K, μ_{34}upregulates mtROS, and HIF-1 inhibits μ_{200}. The dark red region shows the area in which the PSF stabilized model only has the E/M-W/O state. The light red in the bottom left corner near (0,0.1) is the only region in which both models are fully in the E/M-W/O state. The light red on the right is where neither model is in the E/M-W/O state.

Discussion

This work has presented a comprehensive guide to the effects generated by various regulatory links that couple core circuits responsible for the epithelial-mesenchymal transition and the choice of glucose metabolism. We started by considering the activation of individual links and discovered that these can have rather distinct effects. This made it challenging to study the combined effects of simultaneously including several links. This challenge was again compounded by having to consider the external signals that set the parameters of, and thereby bias, the individual EMT and metabolic subsystems and their interaction. We therefore decided to focus primarily on E/M-W/O phenotypes, as we expect that these cells are the most metastatically capable.

Some of our important findings include:

- When the miRNA of the EMT network regulate the metabolic network, the E/M-W/O phenotype can be upregulated with just a single crosstalk. However, when the TFs of the metabolic network regulate the EMT network, a minimum of two crosstalks with opposite effects must be active. Additionally, if crosstalks in both directions are active it is possible to suppress all states except the E/M-W/O phenotype.

- The stabilization of the most plastic E/M-W/O can be facilitated by the addition of "phenotypic stability factors' (PSFs) to the baseline circuit. Interestingly, one can obtain such states even under conditions when the individual core circuits do not generate hybrid states on their own.

- Lastly, to suppress all coupled states except the hybrid E/M-W/O, our results indicate a progression must be followed; starting from an E-O state, metabolic reprogramming can push the state to E-W/O, followed by partial EMT to stabilize the hybrid E/M-W/O state.

Our results suggest that mtROS is critical to the metabolic activation of EMT. In agreement with our results, recent experimental work has posited that mtROS may drive EMT[70], control cancer invasiveness[71,72], and have a much stronger role than noxROS[48][63]. Also, while it is generally accepted that HIF-1 is important to metabolic reprogramming [22] and triggering EMT [9], the connection between HIF-1, mtROS, and cancer aggressiveness has also been suggested [73]. Indeed, our results suggest the mtROS/HIF-1 axis is critical to stabilizing the highly aggressive E/M-W/O state. Additionally, ROS and HIF-1 expression is controlled by the miRNAs of the EMT network, μ_{34} and μ_{200}, confirming the importance of miRNAs in cancer metastasis [74]. Consequently, our results suggest the existence of a feedback loop between μ_{34}, μ_{200}, HIF-1 and ROS may be critical to stabilizing the E/M-W/O state associated with metastasis and tumorigenesis.

In agreement with other studies[30] our findings indicate that all else being equal, undergoing EMT tends to correlate with using additional glycolysis. This result is consistent with a recent study based on published expression data from public databases[67]. The result is somewhat surprising given the widespread impression that primary tumors often exhibit the Warburg effect, possibly because of their need to limit the amount of ATP produced in favor of maximizing growth (see [75] and references therein). However, this finding is consistent with the general idea that moving from E to E/M is connected with increasing stemness, and stem-like capabilities often rely on glycolysis. Resolution of this issue must await a more precise idea of

the phrase ‘all else being equal”. For example, we have ignored external driving of Hif-1 as would clearly occur in hypoxic environments. Mesenchymal cells that reduce proliferation and have to traverse the ECM should switch to more OXPHOS, whereas ones that become quiescent in a hypoxic metastatic niche should favor glycolysis.

In line with the above, this work is merely a first step, and it is quite likely that incorporating additional pathways may be necessary to improve our understanding of the mutual activation between EMT, metabolic reprogramming and other physiological factors. One such factor is NRF2. Coupling the KEAP1-NRF2 pathway to Notch signaling has been connected to the E/M phenotype [43], and NRF2 is also an antioxidant that must be downregulated to increase ROS production [48–50]. Perhaps the metabolic phenotype of NRF2-stabilized E/M cells may correspond to a hybrid W/O phenotype [29]. Additionally, the p53 pathway seems to upregulate noxROS and interfere with EMT [52,53]. Similarly, the E/M-W/O state was stabilized when the Input to SNAIL was modulated confirming the tumor microenvironment and other signals, such as TGF-β and NF-κβ, may be important to generating the E/M-W/O state [77,78]. Therefore, the significance of the mtROS/HIF-1/μ_{200}/μ_{34}/SNAIL feedback loop could be experimentally tested by reducing the antioxidant factor SOD2, inducing hypoxia, and treating the cells with NF-κβ. Overall, the importance of external signaling in our model is in conceptual agreement with a hypothesis by Sciacovelli and Frezza that, in an adverse tumor microenvironment, metabolic reprogramming drives EMT to allow cells to find more favorable metabolic niches[40].

Understanding how the E/M-W/O phenotype is stabilized by the crosstalks of EMT and metabolic reprogramming could be of vital importance to disrupt metastatic processes. Interestingly, the model we have proposed predicts EMT can drive metabolic reprogramming or vice versa, a question that remains unanswered [30–37,40–42]. In both instances the hybrid E/M

and hybrid W/O phenotypes are coupled. A recent study showed EMT may not always be correlated with the Warburg/ OXPHOS metabolic axis, but when the two networks are coupled our model agrees with the identified experimental correlations between high glycolysis metabolism, high or low OXPHOS metabolism, and the E/M state[67]. Our model is consistent, predicting the hybrid E/M state is coupled to high glycolysis/high OXPHOS (hybrid W/O state). Additionally, HIF-1 (a marker of glycolysis) is strongly associated with EMT while AMPK (a marker of OXPHOS) has a much weaker effect, suggesting the E/M state can be stabilized if HIF-1 (glycolysis) is upregulated, as we proposed above. Notably, in its current form, our model is unable to explain the low glycolysis metabolism correlated with EMT. However, extending the model by coupling with glycolysis, glucose oxidation, and fatty acid oxidation metabolic pathways[76] may be able to explain the low glycolysis states of Ref.[67] .

The results of our model suggest that metabolic reprogramming can indeed drive EMT, but metabolic reprogramming does not have to be complete before EMT begins; this allows the most aggressive E/M-W/O phenotype to be stabilized. Further, to ensure only the E/M-W/O state is accessible, the system follows a progression from the E-O state, undergoes metabolic reprogramming while maintaining epithelial characteristics (E-W/O coupled state), begins EMT and stabilizes in the E/M-W/O state. Strikingly, the prevalence of the E/M-W/O state is increased by EMT-metabolism crosstalk regardless of phenotypic availability (i.e., whether the initial system is fully E/M-W/O or only E-O, E-W, M-O, and M-W). Therefore, our current model provides an explanation for metabolic reprogramming driving EMT and should be expanded to explore the opposite process – EMT driving metabolic reprogramming.

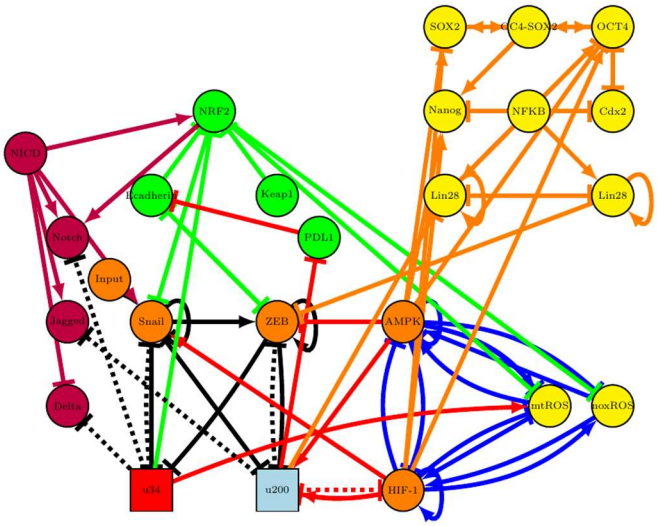

Figure 10: The coupled networks of cancer metastasis. (temporary figure – redrawing it and confirming crosstalks)

The mutual activation of the epithelial-to-mesenchymal transition and metabolic reprogramming stabilizes a highly aggressive E/M-W/O phenotype which may be critical to cancer metastasis. Suppressing all coupled states except the E/M-W/O state requires only three links, suggesting the μ_{34}/μ_{200}/HIF-1/ROS/SNAIL axis is a key subset of crosstalks. When these crosstalks are active, our current model suggests metabolic reprogramming drives EMT. However, previous work suggests EMT can drive metabolic reprogramming[30,79,80]; therefore, the current model should be expanded. As we've noted, studying these networks in isolation is just the first step in understanding how the metastasis is driven by these networks, and incorporating additional networks will be necessary to fully answer this question. For instance, previous studies coupling EMT, stemness, and Notch signaling have shown the various phenotypes associated with therapy resistance, increased metastatic potential, and stem-like properties tend to be correlated[81–83]. However, these couplings also resulted in unexpected behaviors such as the co-localization of hybrid E/M cells[81] and a stemness window that was

tunable[82]. Consequently, studying individual gene regulatory network modules, even in the presence of signals, is unable to give a thorough understanding of the network properties. Therefore, to understand how the various phenotypes are correlated, and potentially identify key regulators, multiple networks and crosstalks should be studied concurrently. One potential coupling would be the EMT network, stemness network, metabolic network, Notch-Jagged signaling, KEAP/NRF2 pathway, and the immune-suppresor PD-L1 (Fig. 10). From this expansive network, we expect therapy resistance, increased metastatic potential, increased invasiveness, hybrid metabolism phenotypes, immune-evasive properties, and stem-like properties would be correlated and key regulators could be identified.

Acknowledgements

This work was supported by National Science Foundation by sponsoring the Center for Theoretical Biological Physics – award PHY-2019745 (JNO, HL) and by awards PHY-1605817 (HL), CHE-1614101 (JNO), and PHY-1522550 (JNO, MG). JNO is a CPRIT Scholar in Cancer Research. MG was also supported by the NSF GRFP no. 1842494.

References

1. Hanahan D. Hallmarks of Cancer: New Dimensions. Cancer Discov. 2022;12(1):31–46.

2. Kalluri R. EMT: When epithelial cells decide to become mesenchymal-like cells. J Clin Invest. 2009;119(6):1417–9.

3. Hay ED. The mesenchymal cell, its role in the embryo, and the remarkable signaling mechanisms that create it. Dev Dynam. 2005;233(3):706–20.

4. Pietilä M, Ivaska J, Mani SA. Whom to blame for metastasis, the epithelial–mesenchymal transition or the tumor microenvironment? Cancer Lett. 2016;380(1):359–68.

5. Talbot LJ, Bhattacharya SD, Kuo PC. Epithelial-mesenchymal transition, the tumor microenvironment, and metastatic behavior of epithelial malignancies. Int J Biochem Mol Biol. 2012 May 18;3(2):117–36.

6. Cho ES, Kang HE, Kim NH, Yook JI. Therapeutic implications of cancer epithelial-mesenchymal transition (EMT). Arch Pharm Res. 2019;42(1):14–24.

7. Lu M, Jolly MK, Levine H, Onuchic JN, Ben-Jacob E. MicroRNA-based regulation of epithelial–hybrid–mesenchymal fate determination. Proc National Acad Sci. 2013;110(45):18144–9.

8. Saitoh M. Involvement of partial EMT in cancer progression. J Biochem. 2018;164(4):257–64.

9. Saxena K, Jolly MK, Balamurugan K. Hypoxia, partial EMT and collective migration: Emerging culprits in metastasis. Transl Oncol. 2020;13(11):100845.

10. Bakir B, Chiarella AM, Pitarresi JR, Rustgi AK. EMT, MET, Plasticity, and Tumor Metastasis. Trends Cell Biol. 2020;30(10):764–76.

11. Pastushenko I, Blanpain C. EMT Transition States during Tumor Progression and Metastasis. Trends Cell Biol. 2018;29(3):212–26.

12. Fustaino V, Presutti D, Colombo T, Cardinali B, Papoff G, Brandi R, et al. Characterization of epithelial-mesenchymal transition intermediate/hybrid phenotypes associated to resistance to EGFR inhibitors in non-small cell lung cancer cell lines. Oncotarget. 2017;8(61):103340–63.

13. George JT, Jolly MK, Xu J, Somarelli J, Levine H. Survival outcomes in cancer patients predicted by a partial EMT gene expression scoring metric. Cancer Res. 2017;77(22):canres.3521.2016.

14. Jolly MK, Tripathi SC, Jia D, Mooney SM, Celiktas M, Hanash SM, et al. Stability of the hybrid epithelial/mesenchymal phenotype. Oncotarget. 2016;7(19):27067–84.

15. Pastushenko I, Brisebarre A, Sifrim A, Fioramonti M, Revenco T, Boumahdi S, et al. Identification of the tumour transition states occurring during EMT. Nature. 2018;556(7702):463–8.

16. Simeonov KP, Byrns CN, Clark ML, Norgard RJ, Martin B, Stanger BZ, et al. Single-cell lineage tracing of metastatic cancer reveals selection of hybrid EMT states. Cancer Cell. 2021;39(8):1150-1162.e9.

17. Dey P, Kimmelman AC, DePinho RA. Metabolic Codependencies in the Tumor Microenvironment. Cancer Discov. 2021;candisc.1211.2020.

18. Warburg O, Wind F, Negelein E. THE METABOLISM OF TUMORS IN THE BODY. J Gen Physiol. 1927;8(6):519–30.

19. Liberti MV, Locasale JW. The Warburg Effect: How Does it Benefit Cancer Cells? Trends Biochem Sci. 2016;41(3):211–8.

20. Ohshima K, Morii E. Metabolic Reprogramming of Cancer Cells during Tumor Progression and Metastasis. Metabolites. 2021;11(1):28.

21. Carvalho TMA, Cardoso HJ, Figueira MI, Vaz CV, Socorro S. The peculiarities of cancer cell metabolism: A route to metastasization and a target for therapy. Eur J Med Chem. 2019;171:343–63.

22. Nagao A, Kobayashi M, Koyasu S, Chow CCT, Harada H. HIF-1-Dependent Reprogramming of Glucose Metabolic Pathway of Cancer Cells and Its Therapeutic Significance. Int J Mol Sci. 2019;20(2):238.

23. Cheng Y, Lu Y, Zhang D, Lian S, Liang H, Ye Y, et al. Metastatic cancer cells compensate for low energy supplies in hostile microenvironments with bioenergetic adaptation and metabolic reprogramming. Int J Oncol. 2018;53(6):2590–604.

24. Jia D, Park JH, Jung KH, Levine H, Kaipparettu BA. Elucidating the Metabolic Plasticity of Cancer: Mitochondrial Reprogramming and Hybrid Metabolic States. Cells. 2018;7(3):21.

25. Yu L, Lu M, Jia D, Ma J, Ben-Jacob E, Levine H, et al. Modeling the Genetic Regulation of Cancer Metabolism: Interplay between Glycolysis and Oxidative Phosphorylation. Cancer Res. 2017;77(7):1564–74.

26. Sancho P, Burgos-Ramos E, Tavera A, Bou Kheir T, Jagust P, Schoenhals M, et al. MYC/PGC-1α Balance Determines the Metabolic Phenotype and Plasticity of Pancreatic Cancer Stem Cells. Cell Metab. 2015;22(4):590–605.

27. Jia D, Paudel BB, Hayford CE, Hardeman KN, Levine H, Onuchic JN, et al. Drug-Tolerant Idling Melanoma Cells Exhibit Theory-Predicted Metabolic Low-Low Phenotype. Frontiers Oncol. 2020;10:1426.

28. Porporato PE, Payen VL, Pérez-Escuredo J, De Saedeleer CJ, Danhier P, Copetti T, et al. A Mitochondrial Switch Promotes Tumor Metastasis. Cell Reports. 2014;8(3):754–66.

29. LeBleu VS, O'Connell JT, Herrera KNG, Wikman H, Pantel K, Haigis MC, et al. PGC-1α mediates mitochondrial biogenesis and oxidative phosphorylation in cancer cells to promote metastasis. Nat Cell Biol. 2014;16(10):992–1003.

30. Jia D, Park JH, Kaur H, Jung KH, Yang S, Tripathi S, et al. Towards decoding the coupled decision-making of metabolism and epithelial-to-mesenchymal transition in cancer. Brit J Cancer. 2021;1–10.

31. Georgakopoulos-Soares I, Chartoumpekis DV, Kyriazopoulou V, Zaravinos A. EMT Factors and Metabolic Pathways in Cancer. Frontiers Oncol. 2020;10:499.

32. Fedele M, Sgarra R, Battista S, Cerchia L, Manfioletti G. The Epithelial–Mesenchymal Transition at the Crossroads between Metabolism and Tumor Progression. Int J Mol Sci. 2022;23(2):800.

33. Burger GA, Danen EHJ, Beltman JB. Deciphering Epithelial–Mesenchymal Transition Regulatory Networks in Cancer through Computational Approaches. Frontiers Oncol. 2017;7:162.

34. Hu Y, Xu W, Zeng H, He Z, Lu X, Zuo D, et al. OXPHOS-dependent metabolic reprogramming prompts metastatic potential of breast cancer cells under osteogenic differentiation. Brit J Cancer. 2020;123(11):1644–55.

35. Sung JY, Cheong JH. Pan-Cancer Analysis Reveals Distinct Metabolic Reprogramming in Different Epithelial–Mesenchymal Transition Activity States. Cancers. 2021;13(8):1778.

36. Choudhary KS, Rohatgi N, Halldorsson S, Briem E, Gudjonsson T, Gudmundsson S, et al. EGFR Signal-Network Reconstruction Demonstrates Metabolic Crosstalk in EMT. Plos Comput Biol. 2016;12(6):e1004924.

37. Feng S, Zhang L, Liu X, Li G, Zhang B, Wang Z, et al. Low levels of AMPK promote epithelial-mesenchymal transition in lung cancer primarily through HDAC4- and HDAC5-mediated metabolic reprogramming. J Cell Mol Med. 2020;24(14):7789–801.

38. Kang X, Wang J, Li C. Exposing the Underlying Relationship of Cancer Metastasis to Metabolism and Epithelial-Mesenchymal Transitions. Iscience. 2019;21:754–72.

39. Kang X, Li C. A Dimension Reduction Approach for Energy Landscape: Identifying Intermediate States in Metabolism-EMT Network. Adv Sci. 2021;2003133.

40. Sciacovelli M, Frezza C. Metabolic reprogramming and epithelial-to-mesenchymal transition in cancer. Febs J. 2017;284(19):3132–44.

41. Huang R, Zong X. Aberrant cancer metabolism in epithelial–mesenchymal transition and cancer metastasis: Mechanisms in cancer progression. Crit Rev Oncol Hemat. 2017;115:13–22.

42. Jiang L, Xiao L, Sugiura H, Huang X, Ali A, Kuro-o M, et al. Metabolic reprogramming during TGFβ1-induced epithelial-to-mesenchymal transition. Oncogene. 2015;34(30):3908–16.

43. Bocci F, Tripathi SC, Mercedes SAV, George JT, Casabar JP, Wong PK, et al. NRF2 activates a partial epithelial-mesenchymal transition and is maximally present in a hybrid epithelial/mesenchymal phenotype. Integr Biol. 2019;11(6):251–63.

44. Luo M, Shang L, Brooks MD, Jiagge E, Zhu Y, Buschhaus JM, et al. Targeting Breast Cancer Stem Cell State Equilibrium through Modulation of Redox Signaling. Cell Metab. 2018;28(1):69-86.e6.

45. Colacino JA, Azizi E, Brooks MD, Harouaka R, Fouladdel S, McDermott SP, et al. Heterogeneity of Human Breast Stem and Progenitor Cells as Revealed by Transcriptional Profiling. Stem Cell Rep. 2018;10(5):1596–609.

46. Jia D, Li X, Bocci F, Tripathi S, Deng Y, Jolly MK, et al. Quantifying Cancer Epithelial-Mesenchymal Plasticity and its Association with Stemness and Immune Response. J Clin Medicine. 2019;8(5):725.

47. Lu M, Jolly MK, Gomoto R, Huang B, Onuchic J, Ben-Jacob E. Tristability in Cancer-Associated MicroRNA-TF Chimera Toggle Switch. J Phys Chem B. 2013;117(42):13164–74.

48. Kovac S, Angelova PR, Holmström KM, Zhang Y, Dinkova-Kostova AT, Abramov AY. Nrf2 regulates ROS production by mitochondria and NADPH oxidase. Biochimica Et Biophysica Acta Bba - Gen Subj. 2015;1850(4):794–801.

49. He F, Ru X, Wen T. NRF2, a Transcription Factor for Stress Response and Beyond. Int J Mol Sci. 2020;21(13):4777.

50. Li N, Muthusamy S, Liang R, Sarojini H, Wang E. Increased expression of miR-34a and miR-93 in rat liver during aging, and their impact on the expression of Mgst1 and Sirt1. Mech Ageing Dev. 2011;132(3):75–85.

51. Bai XY, Ma Y, Ding R, Fu B, Shi S, Chen XM. miR-335 and miR-34a Promote Renal Senescence by Suppressing Mitochondrial Antioxidative Enzymes. J Am Soc Nephrol. 2011;22(7):1252–61.

52. Navarro F, Lieberman J. miR-34 and p53: New Insights into a Complex Functional Relationship. Plos One. 2015;10(7):e0132767.

53. Italiano D, Lena AM, Melino G, Candi E. Identification of NCF2/p67phox as a novel p53 target gene. Cell Cycle. 2012;11(24):4589–96.

54. Chou HL, Fong Y, Wei CK, Tsai EM, Chen JYF, Chang WT, et al. A Quinone-Containing Compound Enhances Camptothecin-Induced Apoptosis of Lung Cancer Through Modulating Endogenous ROS and ERK Signaling. Arch Immunol Ther Ex. 2017;65(3):241–52.

55. Serocki M, Bartoszewska S, Janaszak-Jasiecka A, Ochocka RJ, Collawn JF, Bartoszewski R. miRNAs regulate the HIF switch during hypoxia: a novel therapeutic target. Angiogenesis. 2018;21(2):183–202.

56. Shang Y, Chen H, Ye J, Wei X, Liu S, Wang R. HIF-1α/Ascl2/miR-200b regulatory feedback circuit modulated the epithelial-mesenchymal transition (EMT) in colorectal cancer cells. Exp Cell Res. 2017;360(2):243–56.

57. Byun Y, Choi YC, Jeong Y, Lee G, Yoon S, Jeong Y, et al. MiR-200c downregulates HIF-1α and inhibits migration of lung cancer cells. Cell Mol Biol Lett. 2019;24(1):28.

58. Xu X, Tan X, Tampe B, Sanchez E, Zeisberg M, Zeisberg EM. Snail Is a Direct Target of Hypoxia-inducible Factor 1α (HIF1α) in Hypoxia-induced Endothelial to Mesenchymal Transition of Human Coronary Endothelial Cells*. J Biol Chem. 2015;290(27):16653–64.

59. Chou CC, Lee KH, Lai IL, Wang D, Mo X, Kulp SK, et al. AMPK Reverses the Mesenchymal Phenotype of Cancer Cells by Targeting the Akt–MDM2–Foxo3a Signaling Axis. Cancer Res. 2014;74(17):4783–95.

60. Ohshima J, Wang Q, Fitzsimonds ZR, Miller DP, Sztukowska MN, Jung YJ, et al. Streptococcus gordonii programs epithelial cells to resist ZEB2 induction by Porphyromonas gingivalis. Proc National Acad Sci. 2019;116(17):201900101.

61. Dong T, Zhang Y, Chen Y, Liu P, An T, Zhang J, et al. FOXO1 inhibits the invasion and metastasis of hepatocellular carcinoma by reversing ZEB2-induced epithelial-mesenchymal transition. Oncotarget. 2016;8(1):1703–13.

62. Huang W, Cao J, Liu X, Meng F, Li M, Chen B, et al. AMPK Plays a Dual Role in Regulation of CREB/BDNF Pathway in Mouse Primary Hippocampal Cells. J Mol Neurosci. 2015;56(4):782–8.

63. Jin H, Xue L, Mo L, Zhang D, Guo X, Xu J, et al. Downregulation of miR-200c stabilizes XIAP mRNA and contributes to invasion and lung metastasis of bladder cancer. Cell Adhes Migr. 2019;13(1):236–48.

64. Janin M, Esteller M. Oncometabolite Accumulation and Epithelial-to-Mesenchymal Transition: The Turn of Fumarate. Cell Metab. 2016;24(4):529–30.

65. Zhang Q, Zheng S, Wang S, Wang W, Xing H, Xu S. Chlorpyrifos induced oxidative stress to promote apoptosis and autophagy through the regulation of miR-19a-AMPK axis in common carp. Fish Shellfish Immun. 2019;93:1093–9.

66. Thomson DM, Herway ST, Fillmore N, Kim H, Brown JD, Barrow JR, et al. AMP-activated protein kinase phosphorylates transcription factors of the CREB family. J Appl Physiol. 2008;104(2):429–38.

67. Muralidharan S, Sahoo S, Saha A, Chandran S, Majumdar SS, Mandal S, et al. Quantifying the Patterns of Metabolic Plasticity and Heterogeneity along the Epithelial–Hybrid–Mesenchymal Spectrum in Cancer. Biomol. 2022;12(2):297.

68. Tripathi S, Kessler DA, Levine H. Biological Networks Regulating Cell Fate Choice Are Minimally Frustrated. Phys Rev Lett. 2020;125(8):088101.

69. Farris JC, Pifer PM, Zheng L, Gottlieb E, Denvir J, Frisch SM. Grainyhead-like 2 Reverses the Metabolic Changes Induced by the Oncogenic Epithelial–Mesenchymal Transition: Effects on Anoikis. Mol Cancer Res. 2016;14(6):528–38.

70. Radisky DC, Levy DD, Littlepage LE, Liu H, Nelson CM, Fata JE, et al. Rac1b and reactive oxygen species mediate MMP-3-induced EMT and genomic instability. Nature. 2005;436(7047):123–7.

71. Mori K, Uchida T, Yoshie T, Mizote Y, Ishikawa F, Katsuyama M, et al. A mitochondrial ROS pathway controls matrix metalloproteinase 9 levels and invasive properties in RAS-activated cancer cells. Febs J. 2019;286(3):459–78.

72. Ishikawa K, Takenaga K, Akimoto M, Koshikawa N, Yamaguchi A, Imanishi H, et al. ROS-Generating Mitochondrial DNA Mutations Can Regulate Tumor Cell Metastasis. Science. 2008;320(5876):661–4.

73. SHIDA M, KITAJIMA Y, NAKAMURA J, YANAGIHARA K, BABA K, WAKIYAMA K, et al. Impaired mitophagy activates mtROS/HIF-1α interplay and increases cancer aggressiveness in gastric cancer cells under hypoxia. Int J Oncol. 2016;48(4):1379–90.

74. Babaei G, Raei N, milani AT, Aziz SGG, Pourjabbar N, Geravand F. The emerging role of miR-200 family in metastasis: focus on EMT, CSCs, angiogenesis, and anoikis. Mol Biol Rep. 2021;48(10):6935–47.

75. Tripathi S, Park JH, Pudakalakatti S, Bhattacharya PK, Kaipparettu BA, Levine H. A mechanistic modeling framework reveals the key principles underlying tumor metabolism. Plos Comput Biol. 2022;18(2):e1009841.

76. Jia D, Lu M, Jung KH, Park JH, Yu L, Onuchic JN, et al. Elucidating cancer metabolic plasticity by coupling gene regulation with metabolic pathways. Proc National Acad Sci. 2019;116(9):201816391.

77. Thiery JP, Acloque H, Huang RYJ, Nieto MA. Epithelial-Mesenchymal Transitions in Development and Disease. Cell. 2009;139(5):871–90.

78. Zhang K, Zhaos J, Liu X, Yan B, Chen D, Gao Y, et al. Activation of NF-B upregulates Snail and consequent repression of E-cadherin in cholangiocarcinoma cell invasion. Hepato-gastroenterol. 2011;58(105):1–7.

79. Miyazono K. Transforming growth factor-β signaling in epithelial-mesenchymal transition and progression of cancer. Proc Jpn Acad Ser B Phys Biological Sci. 2009;85(8):314–23.

80. Zhang J, Tian XJ, Xing J. Signal Transduction Pathways of EMT Induced by TGF-β, SHH, and WNT and Their Crosstalks. J Clin Medicine. 2016;5(4):41.

81. Bocci F, Gearhart-Serna L, Boareto M, Ribeiro M, Ben-Jacob E, Devi GR, et al. Toward understanding cancer stem cell heterogeneity in the tumor microenvironment. Proc National Acad Sci. 2018;116(1):201815345.

82. Jolly MK, Jia D, Boareto M, Mani SA, Pienta KJ, Ben-Jacob E, et al. Coupling the modules of EMT and stemness: A tunable 'stemness window' model. Oncotarget. 2015;6(28):25161–74.

83. Bocci F, Jolly MK, George JT, Levine H, Onuchic JN. A mechanism-based computational model to capture the interconnections among epithelial-mesenchymal transition, cancer stem cells and Notch-Jagged signaling. Oncotarget. 2018;9(52):29906–20.